Effect of alumina thickness on Al_2O_3/InP interface with post deposition annealing in oxygen ambient*

Yang Zhuo(杨 卓)†, Yang Jing-Zhi(杨靖治), Huang Yong(黄 永), Zhang Kai(张 锴), and Hao Yue(郝 跃)

State Key Discipline Laboratory of Wide Band-gap Semiconductor Technology, Xidian University, Xi'an 710071, *China*

(Received 21 October 2013; revised manuscript received 24 December 2013; published online 15 May 2014)

In this paper, the effect of alumina thickness on Al_2O_3/InP interface with post deposition annealing (PDA) in the oxygen ambient is studied. Atomic layer deposited (ALD) Al_2O_3 films with four different thickness values (5 nm, 7 nm, 9 nm, 11 nm) are deposited on InP substrates. The capacitance–voltage (*C–V*) measurement shows a negative correlation between the alumina thickness and the frequency dispersion. The X-ray photoelectronspectroscopy (XPS) data present significant growth of indium-phosphorus oxide near the Al_2O_3/InP interface, which indicates serious oxidation of InP during the oxygen annealing. The hysteresis curve shows an optimum thickness of 7 nm after PDA in an oxygen ambient at 500 °C for 10 min. It is demonstrated that both sides of the interface are impacted by oxygen during post deposition annealing. It is suggested that the final state of the interface is of reduced positively charged defects on Al_2O_3 side and oxidized InP, which degrades the interface.

Keywords: Al_2O_3, oxygen annealing, capacitance–voltage measurement, hysteresis curve

PACS: 73.40.Qv, 85.30.De, 61.50.Ah, 61.72.Cc **DOI:** 10.1088/1674-1056/23/7/077305

1. Introduction

As silicon technology is reaching its fundamental physical limit, various devices, which are based on high electron mobility III-V semiconductor materials, have been fabricated in the past two decades, such as: high electron mobility transistors (HEMT's),[1] heterojunction bipolar transistors (HBT's),[2,3] heterostructure insulated gate FET's (HIGFET's),[4] and p-channel FET's.[5] Research on mentaloxide semiconductor field-effect transistors (MOSFETs) has also been carried out in recent years. Among the III-V materials, InP has received much attention for its high mobility and frequency property. A critical issue for III-V MOSFETs is the high defect density between the III-V material and the high-*k* dielectric layer,[6] which leads to a shallow, buried channel structure with an InGaAs channel and an InGaP/InP barrier layer.[7] Although the InP barrier layer separates the high-*k* dielectric layer from the InGaAs layer, there still exists a high defect density, which will affect the subthreshold swing and the threshold voltage.[8] Since rapid temperature annealing (RTA) is known as a common method to improve the interface, research has been conducted on the effect of post deposition annealing (PDA) in N_2[7] and H_2[9] ambient. In addition, oxygen annealing has been proven to be an effective method to reduce the defects in Al_2O_3.[10] However, little work has been done to discuss how alumina thickness affects the InP/Al_2O_3 interface with post deposition annealing in oxygen ambient. In this paper, we show the electrical performance of n-InP metal-oxide-semiconductor (MOS) capacitors with different Al_2O_3 thickness values (5 nm, 7 nm, 9 nm, 11 nm) after post deposition annealing in oxygen ambient. Detailed analysis of the X-ray photoelectronspectroscopy (XPS) results and a model extracted from *C–V* measurements are presented.

2. Fabrication and measurement

MOS capacitor devices on n-InP substrates (S doped; mobility∼1700) with Al_2O_3 dielectric were fabricated through the following process. First, a SiO_2 layer (2000 Å) was grown on the back of the InP substrates as a protection layer by plasma enhanced chemical vapor deposition (PECVD). The wafers were cleaned by a standard degreasing process, including sequential immersion in acetone andethanol for 5 min each. Then, the wafers were immersed in hydrochloric acid (HCl:H_2O=1:26) for 3 min and in ammonia water for 5 min to remove the native oxide layer in InP surface. The different Al_2O_3 layers of 5 nm, 7 nm, 9 nm, 11 nm in thickness were then deposited on InP substratesat 300 °C by ALD technology, respectively. Post-deposition annealing was employed in oxygen ambient for 10 min at 500 °C. The MOS structure pattern was determined by photoetchingusing SUSS MA6. Photoetching was followed by gate metal sputtering. DP650 was used to sputter 200-Å Ni and 2000-Å Au. The acetone and ethanol were used again to deal with the unrequired photoresist. The last step was post-metal annealing (PMA) at 400 °C for 30 s in N_2 ambient after the removal of the photoresist.

Cascade 12000 *C–V* measurement system with long integration time was used to accomplish *C–V* measurements for

*Project supported by the National Natural Science Foundation of China (Grant No. 61204006), the Fundamental Research Funds for the Central Universities, China (Grant No. K50511250002), and the National Key Science and Technology Special Project, China (Grant No. 2008ZX01002-002).

†Corresponding author. E-mail: sdyblue@163.com

© 2014 Chinese Physical Society and IOP Publishing Ltd

the four samples. Two additional samples, each with a 5-nm-thick Al_2O_3 layer, were fabricated: one with a 500 °C PDA for 10 min annealing in oxygen ambient and another without PDA. These two samples were characterized at Beijing University of Chemical Technology for XPS measurement.

3. Results and discussion

Figure 1 shows the room-temperature frequency-dependent *C*–*V* curves of the four samples. Obvious frequency dispersions are present in both the accumulation region and the depletion region, which indicates a high density of interface traps. Frequency dispersion in the accumulation region is often attributed to series resistance, which comes from cabling, substrates, and contacts. However, frequency dispersion is due to series resistance has ω^{-2} dependence,[7] which is not observed here. Therefore, series resistance is not responsible for the dispersion.

A model has been introduced to explain the frequency dispersion in the accumulation region.[11] The disorder induced gap state (DIG) model attributes this frequency dispersion to the tunneling of carriers into a disordered region. The tunneling of carriers is caused by oxidation of the III-V substrate.[12,13] Table 1 gives the calculated results of frequency dispersion for different alumina thickness values, showing a negative correlation between frequency dispersion and alumina thickness. As the alumina thickness grows, the chance for oxygen ambient to oxidize InP substrate decreases. The calculations in Table 1 coincide with the values from the DIG model, which indicates that the oxidation on the InP side is considered to be responsible for the dispersion in the accumulation region.

Table 1. Frequency dispersions for different alumina thickness values.

V_{gs}/V	5 nm/%	7 nm/%	9 nm/%	11 nm/%
0.8	13.56	7.43	6.97	6.20
2.5	19.25	9.12	9.15	8.81

Moreover, strong inversion is suppressed in nearly all the samples, except in the sample with 7-nm-thick Al_2O_3 layer after annealing in oxygen ambient. This is different from what happens to the curves of Al_2O_3/InP samples each with 10-nm-thick Al_2O_3 layer annealing in N_2 ambient,[7] which show strong inversion at 1 kHz.

The chemical composition of the Al_2O_3/InP interface and the effect of O_2 PDA are investigated by XPS for individual samples, each with a 5-nm Al_2O_3 layer. Figures 2 and 3 show the core level spectra of In 3d and O 1s for a 5-nm-thick Al_2O_3 layer on an InP substrate. All peaks are fitted by XPSPEAK software and the data are processed by Origin 8. The In 3d

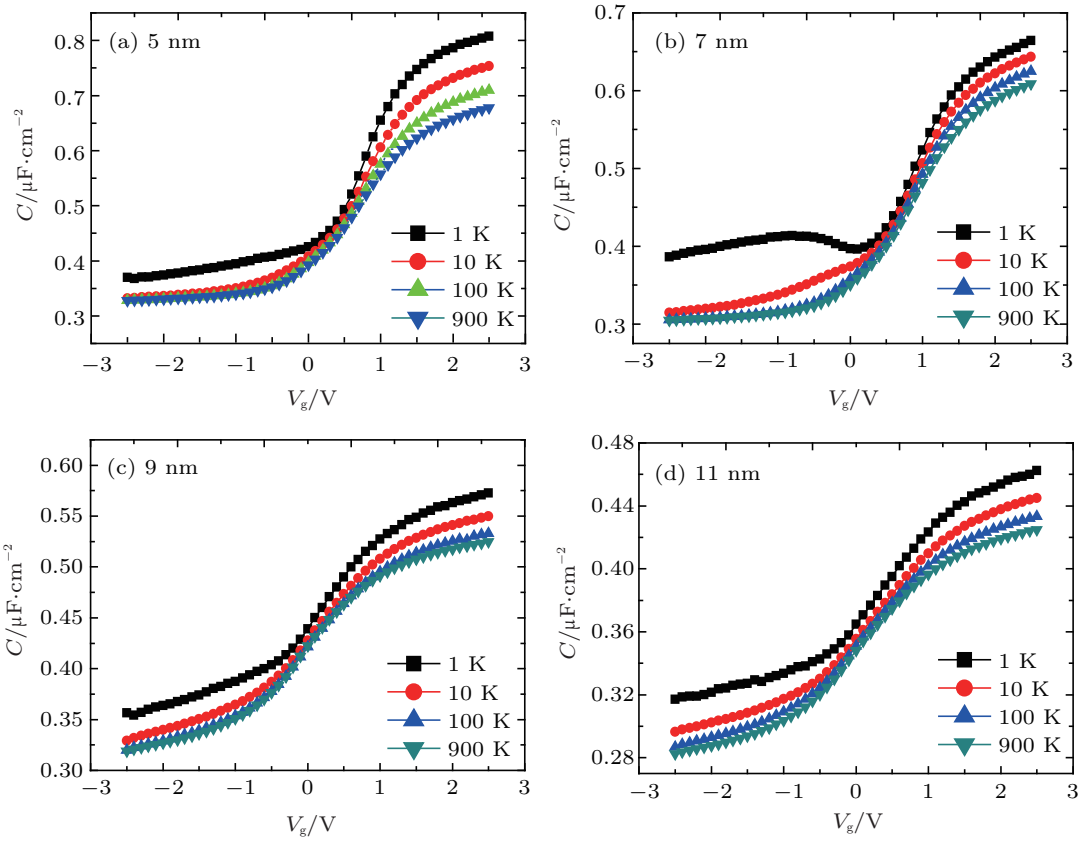


Fig. 1. (color online) Room temperature multi-frequency *C*–*V* characteristics for samples with different thickness values of Al_2O_3 layer: (a) 5 nm, (b) 7 nm, (c) 9 nm, and (d) 11 nm.

core level spectra in Fig. 2 show the peaks of In–O (probably In_2O_3), a combination of $In(PO_3)_3$ and $InPO_4$, and an $InPO_x$. The binding energies of the three peaks apart from the bulk InP peak are 0.5 eV, 1.1 eV, and 1.7 eV, respectively. According to the O 1s core level spectra in Fig. 3, a peak with a binding energy of 532 eV is assigned to Al_2O_3 overlapping with bridging O ions in InP_xO_y. The peak with a binding energy of 533 eV is detected as non-bridging O ions in InP_xO_y, and the peak with a binding energy of 533.8 eV is assigned to a P_2O_5 state overlapping with Al–OH bonding.[7]

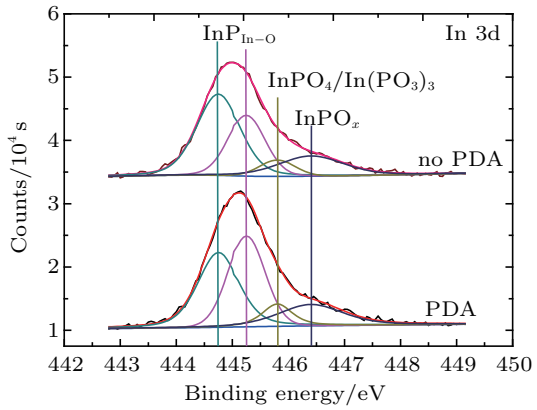


Fig. 2. (color online) XPS results of the In 3d spectra for Al_2O_3/InP interfaces in the cases without PDA and with oxygen PDA.

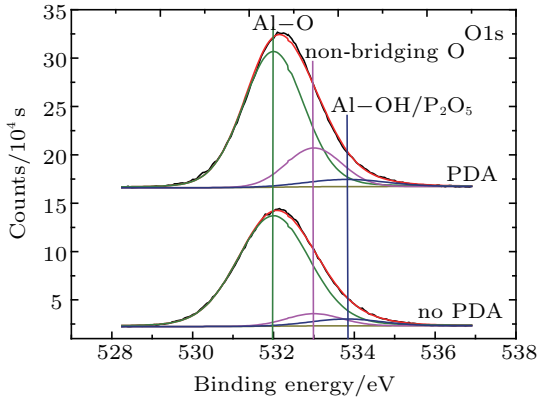


Fig. 3. (color online) XPS results of the O 1s spectra for Al_2O_3/InP interfaces in the cases with and without oxygen PDA.

According to the changes of the peaks in Fig. 2, significant increases of In–O and $InPO_4/In(PO_3)_3$ after annealing in oxygen ambient are presented. The peak of In–O replaces the original bulk In–P peak as a new highest peak, which indicates the serious oxidation of InP and the existence of a new layer of indium oxide and phosphorus oxide. In Fig. 3, the peak of non-bridging O ions in InP_xO_y shows a remarkable increase after annealing, demonstrating the generation of InP oxide layer once again.

Figure 4 shows the hysteresis curves of the four samples with Al_2O_3 layers of different thickness values. It is found that the sample with a 7 nm-thick Al_2O_3 layer shows the best hysteresis property, suggesting a non-linear correlation between the magnitude of hysteresis and the alumina thickness. Since the magnitude of hysteresis is due to the trapped charges injected from the substrate,[14] border traps in Al_2O_3 are considered to be responsible for the hysteresis.[15] A formula is given below to show the relationship between the density of border traps and the magnitude of hysteresis at the flat band voltage

$$N_{\rm bt} = \frac{C_{\rm ox}\Delta V_{\rm mg}}{Aq}, \tag{1}$$

where $N_{\rm bt}$ is the density of border traps, $C_{\rm ox}$ is the capacitance of oxide, A is the area of the MOS capacitor, q is the electrics charge, and $\Delta V_{\rm mg}$ is the difference between the forward curve and backward curve with a frequency of 1 MHz at the flat band voltage.[15] According to this expression, a non-linear correlation between the density of border traps and the alumina thickness is presented, in which there exists an optimum alumina thickness value for the lowest density of border trap.

According to the formula above and the observed measurements, we divide the effect of Al_2O_3 thickness into two cases. One is the case where the alumina deposited by ALD with TMA and H_2O is placed in an aluminum rich ambient during deposition, leading to lots of defects such as Al_i or V_O, which is positively charged.[16] These positively charged defects near the InP/Al_2O_3 interface can easily capture the electrons injected from the n-InP substrate, which contributes to the magnitude of the hysteresis. During the annealing, however, plenty of oxygen ions in the ambient will fill the oxygen vacancy, bond with Al_i and neutralize the defects, hence reducing the magnitude of hysteresis. As the thickness of Al_2O_3 increases, the permeation of oxygenions into the alumina layer turns harder. By means of O isotope, Krug *et al.*[17] have proved that the ambient gas is mainly incorporated in the near-surface region, entering into the structure in the way of decreasing with depth increasing. In addition, a model has been developed for the diffusion of oxygen atoms in a Al_2O_3 film,[18] which could be used here to describe the oxygen ion diffusion in this case.

A phenomenological definition of the diffusion coefficient D_β is given by

$$D_\beta = \lim_{t\to\infty} \frac{|\Delta \boldsymbol{r}|^2}{t^\beta}, \tag{2}$$

where $|\Delta \boldsymbol{r}|^2 = |\boldsymbol{r} - \boldsymbol{r}'|^2$ is the variance of the spatial distribution of the diffusing quantity, $W(x,t)$ is the possibility that the atom moves from site x to site x' at time t.

By defining $D(x,t) = (\partial x^2/\partial t)W(x,t)$, the probability distribution of finding a distributing atom at site x and time t, defined as $p(x,t)$, can be given below

$$\frac{\partial P}{\partial t} = \frac{\partial}{\partial x}\left[D(x,t)\frac{\partial P}{\partial X}\right]. \tag{3}$$

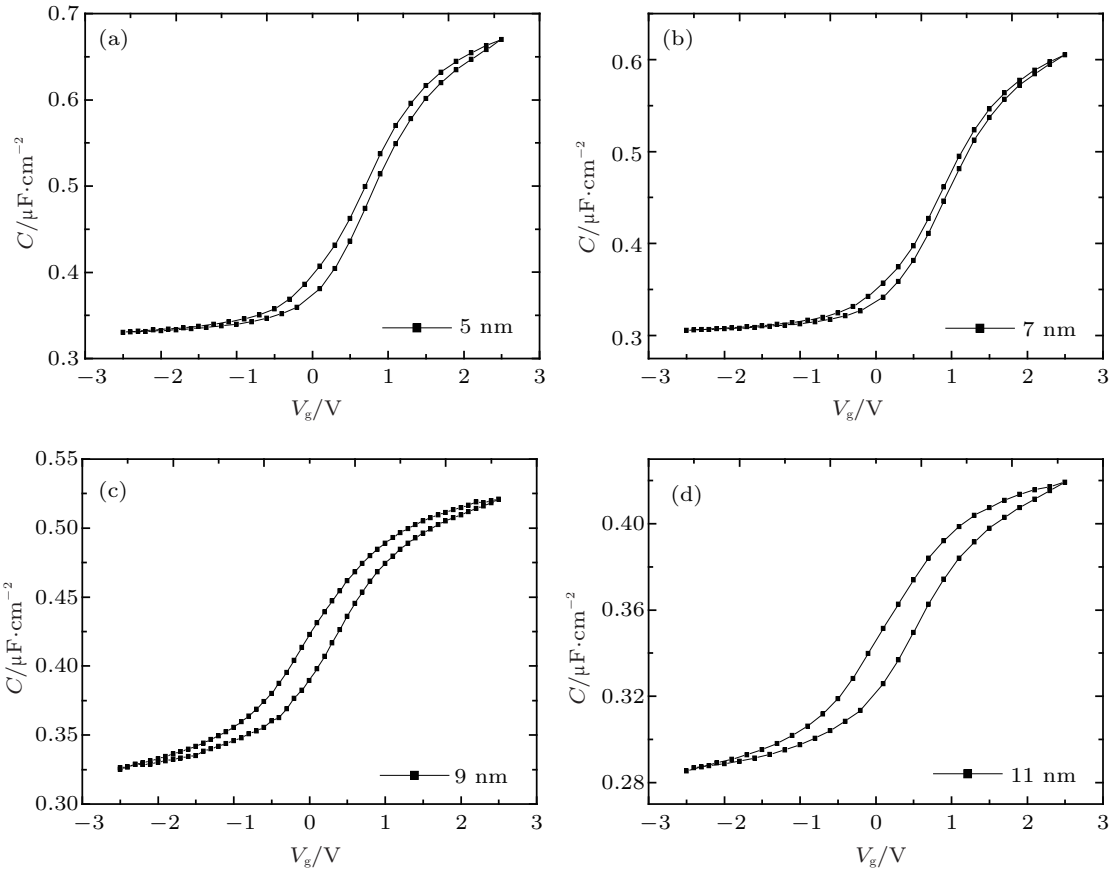


Fig. 4. Hysteresis measurements for samples with different thickness values of Al_2O_3 layer: (a) 5 nm, (b) 7 nm, (c) 9 nm, and (d) 11 nm.

In this case, however, time is constant and depth is the only dimension, that is, $D(x,t) = D(x)$, equation (3) can be transformed into the following equation:

$$\rho(x) = \frac{1}{\int \mathrm{d}x'}, \tag{4}$$

where x' is the next position to which the atom moved from x.

According to Eq. (4), the longer a distance the oxygen atom moves, the more deeply it gets into the alumina layer, leading to a lower spatial density $\rho_O(x)$. Here, $\rho_O(x)$ is the spatial density of oxygen atoms in the x position. Equation (4) gives the reciprocal relationship between alumina layer thickness and the oxygen spatial density at the back surface of the alumina layer.

Since less oxygen ions permeate near the surface with alumina growing thicker, the improvement of oxygen ambient in Al_2O_3 layer becomes weak, resulting in a positive correlation between Al_2O_3 thickness and the magnitude of hysteresis. According to Figs. 2 and 3, the InP side of InP/Al_2O_3 is seriously oxidized during the oxygen annealing, forming a layer of oxidizing indium and phosphorus oxide between the InP layer and the Al_2O_3 layer. This can be explained from the change of Gibbs free energy. The Gibbs free energy of formation per O atom −527 kJ/mol for Al_2O_3 is higher than those for indium and phosphorus oxides (In_2O_3: −958.1 kJ/mol; P_2O_5: −3078.1 kJ/mol). According to the research results given by Dong *et al.*,[19] Al_2O_3/InP interface, upon annealing may lead to Indium atoms diffusion into Al_2O_3 and enhance the phosphorus-oxide richness at the interface. The extra defects brought by the newly formed oxide layer provide more chances for the electrons to be injected from the substrate. Since it is more difficult for ambient oxygen atoms to oxidize Al_2O_3/InP interface with Al_2O_3 thickness growing, a negative correlation between the thickness of Al_2O_3 and the magnitude of hysteresis is suggested. Above all, the effect of alumina thickness on the InP/Al_2O_3 interface after oxygen annealing is assumed to be a combination of both cases, thus the existence of an optimum thickness for the Al_2O_3 layer.

4. Conclusion

Investigation for the effect of alumina thickness on Al_2O_3/InP interface with PDA in an oxygen ambient is conducted in this paper. A significant increase in indium-phosphorus oxidation state after post deposition annealing is observed from the XPS curve. The frequency dispersion given by *C–V* measurement shows a negative correlation with the thickness of the alumina layer, indicating that a relatively thick oxide layer improves the property of the frequency dispersion. The DIG model is introduced to explain this correlation. In addition, the suppression of inversion is observed in the *C–V* curve. The hysteresis measurement shows an opti-

mum alumina thickness of 7 nm where the magnitude of hysteresis is the lowest among the four samples. The effect of alumina thickness on the magnitude of hysteresis is divided into two parts, in which two opposite effects of oxygen annealing on hysteresis are considered and the combination of these two parts finally determines the observable hysteresis property. Since only one annealing condition of oxygen annealing is discussed here, the optimal thickness of Al_2O_3 is expected to change with the condition, which remains to be studied later.

References

[1] Zhang K, Cao M Y, Lei X Y, Zhao S L, Yang L Y, Zheng X F, Ma X H and Hao Y 2013 *Chin. Phys. B* **22** 097303

[2] Zheng J J, Zhang G L, Guo Y X, Li X P and Chen W J 2007 *Chin. Phys.* **16** 1407

[3] Ge J, Liu H G, Su Y B, Cao Y X and Jin Z 2012 *Chin. Phys. B* **21** 058501

[4] Chan Y J, Pavlidis D, Razeghi M, Omnes F and Defour M 1989 *Inst. Phys. Conf. Ser.* **106** 619424

[5] Chan Y J, Pavlidis D, Razeghi M, Jaffe M and Singh J 1988 *Inst. Phys. Conf. Ser.* **96** 459

[6] Xuan Y, Wu Y Q, Lin H C, Shen T and Ye P D 2007 *IEEE Electron Device Lett.* **28** 935

[7] Galatage R V, Dong H, Zhernokletov D M, Brennan B and Hinkle C L 2013 *Appl. Phys. Lett.* **102** 132903

[8] Benbakhti B, Ayubi-Moak J S, Kalna K, Lin D, Hellings G, Brammertz G, Meyer K D, Thayne I and Asenov A 2010 *Microelectron. Reliab.* **50** 360

[9] Liu Z G, Sun X, Yang J, Cui S R, Chen C Y, Chang-Liao K S and Ma T P 2011 *Appl. Phys. Lett.* **99** 222104

[10] Ren C, Yang H, Han D D, Kang J F, Liu X Y and Han R Q 2003 *Chin. J. Semi.* **24** 1109

[11] Hinkle C L, Galatage R V, Zhernokletov D M, Dong H, Anwar S R M, Brennanl B, Wallace R M and Vogel E M 2013 223*rd ECS Meeting*, May 12–16, 2013, Toronto, Canada, p. 768

[12] Sonnet A M, Hinkle C L, Heh D, Bersuker G and Vogel E M 2010 *Trans. Electron Devices* **57** 2599

[13] Hasegawa H and Sawada T 1980 *Trans. Electron Devices* **27** 1055

[14] DalapatiG K, Tong Y, Loh W Y, Mun H K and Cho B J 2007 *Trans. Electron Devices* **54** 1831

[15] Bhat N and Saraswat K C 1998 *J. Appl. Phys.* **84** 2722

[16] Weber J R, Janotti A and van de Walle C G 2011 *J. Appl. Phys.* **109** 033715

[17] Krug C, E B O da Rosa, R M C de Almeida, Morais J, I J R Baumvol, T D M Salgado and F C Stedile 2000 *Phys. Rev. Lett.* **85** 4120

[18] R M C de Almeida and I J R Baumvol 2003 *Surf. Sci. Rep.* **49** 1

[19] Dong H, Cabrera W, Galatage R V, Santosh K C, Brennan B, Qin X, McDonnell S, Zhernokletov D, Hinkle C L, Cho K and Chabal Y J 2013 *Appl. Phys. Lett.* **103** 061601